AAPS PharmSciTech, Vol. 19, No. 7, October 2018 (© 2018)
DOI: 10.1208/s12249-018-1120-2

Research Article

Evaluating the Accelerated Blood Clearance Phenomenon of PEGylated Nanoemulsions in Rats by Intraperitoneal Administration

Yuqing Su,[1] Mengyang Liu,[1] Kaifan Liang,[1] Xinrong Liu,[1] Yanzhi Song,[1,2] and Yihui Deng[1,2]

Received 17 April 2018; accepted 2 July 2018; published online 5 September 2018

Abstract. The accelerated blood clearance (ABC) phenomenon is induced by repeated intravenous injection of stealth polyethylene glycol (PEG) nanocarriers and appears as the alteration of the pharmacokinetics and biodistribution of the second administration. Nevertheless, there is no any report about the ABC phenomenon induced by intraperitoneal administration of PEGylated nanocarriers. In this study, we firstly observed whether the ABC phenomenon is induced with PEGylated nanoemulsion at the dose of 0.5~100 μmol phospholipid·kg^{-1} by intraperitoneal/intravenous injections in rats. The PEG (molecule weight, 2000)-modified nanoemulsions PE-B and PE in which fluorescence indicator dialkylcarbocyanines (DiR) is encapsulated by PE-B were prepared for this work. The pharmacokinetics of the first injected PE *via* veins or peritoneal cavity features different variation trends. Moreover, the tissue distributions (*in vivo* or *in vitro*) of the first injected PE by intraperitoneal injection reveals that the PE gains access to the whole lymphatic circulatory system. Furthermore, our results demonstrate that the ABC phenomenon can be induced by intraperitoneal administration PE-B and present obvious changes with varying PE-B concentration 0.5~100 μmol phospholipid·kg^{-1}. Moreover, an interesting point is that the ABC phenomenon induced by intraperitoneal injected PE-B can be significantly inhibited by intraperitoneal pre-injection of distilled water. For understanding this issue clear, we studied the production of anti-PEG IgM and the characteristic morphologies of immune cells. We observed that the mast cells in peritoneal cavity exhibit rapid depletion in response to the intraperitoneal pre-injection of distilled water, while the anti-PEG IgM secretes at the same level.

KEY WORDS: PEGylated emulsions; ABC phenomenon; intraperitoneal injection; anti-PEG IgM; mast cells.

INTRODUCTION

Over the last few decades, nanocarriers have drawn considerable attention due to their wide application potentiality as carrier systems for targeted drug delivery (1–3). The most successful approach to enhancing nanocarriers delivery has been, so far, to attach countless lipid-conjugated polyethyleneglycol (PEG) to the surface of the nanocarriers, through a technique called PEGylation (4). PEGylation is able to markedly reduce the uptake in both the extent and rate of nanocarriers by the mononuclear phagocyte system (MPS) and, as a result, PEGylation nanocarriers can feature improved stability, circulation time, therapeutic effects, and passive targeting ability on tumoral tissues (5). With these prominent advantages, PEGylation nanoparticles are widely employed for various clinical or laboratoral applications.

Nevertheless, an unexpected immunogenic response, the alleged accelerated blood clearance (ABC) phenomenon, has been exposed. In this phenomenon, the circulation time of a second dose of PEGylated liposomes is significantly decreased upon repeatedly injected *in vivo* because of an enhanced hepatic accumulation, and thusly, this immune problem can reduce the therapeutic efficacy of the encapsulated active ingredients (6–10). Furthermore, this phenomenon was originally observed with PEGylated liposome, which until now has been extensively reappraised using PEG-containing polymeric nanoparticles (11,12), polymeric micelles (13,14), *etc.* Over the years, this abnormal immune response has attracted a great deal of attention because it has serious implications for a further improved utility of PEGylated nanocarriers.

Up to now, despite extensive studies on the ABC phenomenon by some groups, the mechanism governing this phenomenon is still not fully understood. The most

Electronic supplementary material The online version of this article (https://doi.org/10.1208/s12249-018-1120-2) contains supplementary material, which is available to authorized users.

[1] School of Pharmacy, Shenyang Pharmaceutical University, 26 Huatuo Road, Benxi, 117004, People's Republic of China.
[2] To whom correspondence should be addressed. (e–mail: songyanzhi@syphu.edu.cn; dengyihui@syphu.edu.cn

compelling theory suggests that this phenomenon is a result of incremental splenic secretion of anti-PEG IgM (15–18). Specifically, the first injected PEGylated nanocarriers, which play the part of TI-2 antigens (19), induce the splenic B cells which produce anti-PEG IgM; these antibodies then bind to the second administrated PEGylated liposomes, and subsequently the complement is activated; finally, the uptake of the opsonized nanoparticles by resident hepatic macrophages increases (20–22). Moreover, our previous study demonstrated that the regional lymph nodes also have significant effect on the induction of the ABC phenomenon (23). Up to now, many factors have been reported for the influence of the ABC phenomenon, such as the physicochemical properties (24) of PEGylated carriers, the injection dose, or time interval between administration *via* the intravenous/subcutaneous injections (23,25). Compared with the intravenous and subcutaneous injections, the intraperitoneal injection of chemotherapeutics which shows pharmacokinetic advantages is an important cancer therapy method on the clinical (26–28). Moreover, two nanoparticle formulations, NanoTaX® (29) and Abraxane® (30), have been evaluated for the intraperitoneal therapy in the phase I clinical trials in humans. Furthermore, a number of the drug delivery strategies, such as PEG-containing microspheres, nanoparticles, and liposomes, have been investigated to optimize the intraperitoneal therapy (31–33). However, there are no reports assessing the ABC phenomenon using intraperitoneal administration method, while intravenous and subcutaneous injection methods have been widely used to investigate this phenomenon. Hence, it is necessary to investigate whether the ABC phenomenon can be induced by PEGylated nanocarriers by intraperitoneal administration.

In this work, we firstly study the ABC phenomenon of PEGylated nanoemulsions by intraperitoneal administration method in rats. In detail, the PEGylated nanoemulsions PE-B and PE were prepared and their physical properties such as size, morphologies, *zeta* potential, encapsulation efficiency, and DiR release were characterized. The pharmacokinetics and tissue distribution of the first injected PE were analyzed. By intravenous/intraperitoneal injection methods, we evaluated the ABC phenomenon induced by PE-B nanoemulsions with different concentrations. Furthermore, we found that the ABC phenomenon can be markedly inhibited by intraperitoneal pre-injection of sterile water method. For understanding this interesting issue, we measured the production of anti-PEG IgM before and after intraperitoneal pre-injection of sterile water, and for observing the changes caused by pre-injected sterile water, the characteristic morphologies of immune cells in peritoneal cavity were studied in detail. We consider that this work may be clinically useful for combination therapy of PEGylated particles with different injection routes such as intravenous and intraperitoneal injections.

MATERIALS AND METHODS

Materials and Animals

Materials are listed as follows:

Egg phosphatidylcholine (E80) was purchased from the Lipoid GmbH company (Germany); medium-chain triglycerides (MCT) was purchased from the Beiya Medicated Oil company (China); 1,2-distearoyl-sn-glycero-3-phosphoethanolamine-n-[me-thoxy(polyethylene glycol)-2000] ($mPEG_{2000}$-DSPE) was purchased from the Genzyme company (USA); dialkylcarbocyanines (DiR) was purchased from the AAT Bioquest company (USA); sodium dodecyl sulphate (SDS), tris salt, and o-phenylenediamine were purchased from the Sigma-Aldrich company (USA); bovine serum albumin (BSA) was purchased from the Biosharp company (Korea); rabbit anti-rat IgM was purchased from the Beijing Biosynthesis Biotechnology company (China); 50% (*m/v*) glucose (50%Glu) and 5% (*m/v*) glucose (5%Glu) were purchased from the Nanjiang Pharmacy industry (China). The acronyms used in this paper are summed up in Table I.

Wistar rats (male, 180–200 g for each rat) were bought from the Experimental Animal Center of Shenyang Pharmaceutical University (Benxi, Liaoning, China). In accordance with the guidance of the Animal Welfare Committee of Shenyang Pharmaceutical University, all animal experimental procedures were carried out (NIH publication no. 85-23, revised in 1985).

Pharmacokinetics and the ABC Phenomenon

In order to study the pharmacokinetics of injected PE *via* intravenous or intraperitoneal approaches, 12 rats were divided into two groups ($n = 6$). The PE at 5 μmol phospholipid·kg^{-1} was injected *via* the tail vein or peritoneal cavity, respectively. At selected time points, 0.083, 0.25, 0.5, 1, 2, and 4 h, after the injection, 0.5 mL blood samples were collected from the marginal veins of eye and centrifuged to obtain the plasma (4500 rpm, 10 min). For studying the ABC phenomenon, 54 rats were divided into nine groups ($n = 6$). One of them received 5%Glu was treated as the control group. In four groups, the PE-B at a dose of 0.5, 5, 50, and

Table I. Acronyms Used in Manuscript

Abbreviation	Full term
MPS	Mononuclear phagocyte system
PEG	Polyethylene glycol
$mPEG_{2000}$-DSPE	1,2-Distearoyl-sn-glycero-3-phosphoethanolamine-n-[me-thoxy(polyethylene glycol)-2000]
ABC	Accelerated blood clearance
DiR	Dialkylcarbocyanines
MCT	Medium-chain triglycerides
PE-B	Blank nanoemulsions covered with 9%mol $mPEG_{2000}$-DSPE
PE	PE-B with the DiR in the oil phase (MCT)
TEM	Transmittance electron microscopy
SDS	Sodium dodecyl sulfate
PBS	Phosphate buffer saline
EE	Encapsulation efficiency
$AUC_{(0-\infty)}$	Area under the curve from time zero to infinity after the dose
C_{max}	The maximum concentration
%ID	% injection dose
BSA	Bovine serum albumin
Glu	Glucose
i.v.	Intravenous injection
i.p.	Intraperitoneal injection

100 μmol phospholipid·kg^{-1} were administrated *via* the tail vein, respectively. In the remaining four groups, the PE-B at a dose of 0.5, 5, 50 and 100 μmol phospholipid·kg^{-1} were injected intraperitoneally, respectively. Seven days later, all groups were given 5 μmol phospholipid·kg^{-1} of the PE through the tail vein. After this injection, 0.5 mL blood samples were collected from the orbital venous at selected post-injection time points (0.083, 0.25, 0.5, 1, 2, and 4 h) and centrifuged to obtain plasma (4500 rpm, 10 min). The treatment method of the plasma sample containing DiR was as follows: add 100 μL plasma samples into 900 μL ethyl alcohol; vortex the entire mixture for 5 min, and then centrifuge the mixture at 10,000 rpm for 10 min; a further 10 min was applied to recentrifuge the supernatant (600 μL) at 10,000 rpm; add 200 μL the final supernatant into 96-well plates to analyze the DiR plasma concentration by using a microplate reader (Bio-Rad Laboratories, Hertfordshire, UK). Seven hundred fifty millimeter (excitation) and 790 nm (emission) were the detection wavelengths. The pharmacokinetic values, $AUC_{(0-\infty)}$ and C_{max}, were measured by the DAS pharmacokinetic software (2.0 version).

The Effect of the Intraperitoneal Pre-injection of Sterile Water on the ABC Phenomenon

For the first injections, 18 rats were divided into three groups ($n = 6$). One of them was pre-intraperitoneally injected with 5%Glu was treated as the control group (54 mL kg^{-1}). In the other two groups, 54 mL kg^{-1} sterile water was intraperitoneally administered. After 2 days, rats received either an intraperitoneal or intravenous injection containing PE-B. Seven days later, PE (test nanoemulsions, 5 μmol phospholipid·kg^{-1}) were intravenously injected. After this, 0.5 mL blood samples were collected at the time points 0.083, 0.25, 0.5, 1, 2, and 4 h post-injection, through orbital vein and centrifuged to obtain plasma (4500 rpm, 10 min). The plasma sample processing was performed as described in the "Pharmacokinetics and the ABC Phenomenon" of the "MATERIALS AND METHODS" section. The extent of the ABC phenomenon was described using the ABC index (the $AUC_{(0-\infty)}$ mean value of the second dose/the $AUC_{(0-\infty)}$ mean value of the first dose).

Statistical Analysis

The data are shown as the means ± standard deviation. The statistical analysis was performed by using a two-tailed unpaired Student's *t* test with the SPSS 16.0 software (IBM, New York, USA). Statistical significance was set at $p \geq 0.05$, $^{*}p < 0.05$, $^{**}p < 0.01$, and $^{***}p < 0.001$. $^{*}p < 0.05$ was deemed as statistically significant.

RESULTS

The Characteristics of the PEGylated Nanoemulsions

In this study, some physical properties of the PE-B and PE were characterized such as the diameters, morphologies, *zeta* potentials, EE, and DiR release. The detailed experiment methods are described in the Electronic Supplementary Information. The mean diameter of the PE-B is 139.3 ± 3.7 nm, with a narrow size distribution (P.I., 0.1692 ± 0.023). Compared with the PE-B, the average size of the PE (loading the DiR into the PE-B) increases slightly to 147.3 ± 4.2 nm (Fig. 1a). Surface morphologies of the PE-B and PE were identified by a transmission electron microscope (TEM). The TEM images of the PE-B and PE are shown in Fig. S1 in the "Electronic Supplementary Information" and Fig. 1b, respectively. As shown in Fig. 1b, the PE particles present as homogeneous spheres and possess a mean diameter of approximately 140 nm, which agrees with the above average size. As to the *zeta* potentials, Fig. 1a shows that the PE-B and PE are negatively charged, with *zeta* potentials of about − 29.82 ± 3.19 mV and − 26.17 ± 2.85 mV, respectively. The electrostatic repulsion among the nanoemulsions together with the hydration shell formed by PEG maintains a stable state of the PE-B and PE. Figure 1c reveals that the release kinetics of the PE *in vitro* obeys the Ritger-Peppas equation ($R^2 = 0.9818$) and only less than 7% DiR is released from the PE in 48 h. In addition, our previous works show that the DiR is deemed superior in the study of the ABC phenomenon because DiR which is a near-infrared fluorescence dye possesses convenient characteristic on the analytical detection with high sensitivity (34). Moreover, the mean value of the EE (%) of the PE is 98.9%. Hence, the PE-B and PE are qualified candidates of nanoemulsions for the research of the ABC phenomenon.

Pharmacokinetics of the Intravenous/Intraperitoneal Administered PE

The PE was injected through the tail vein or peritoneal cavity at a dose of 5 μmol phospholipid·kg^{-1}. As shown in Fig. 2, the concentration distribution at different timed was analyzed. Figure 2a reveals that the concentration of the intraperitoneal administrated PE increases first and then gradually decreases, while the concentration of the intravenous injected PE experiences a continual decrease. At time 4 h after the intraperitoneal injection, the PE blood concentration reaches maximum value 6.798 ± 1.172 %ID mL^{-1}. The $AUC_{(0-\infty)}$ values of the intravenous and intraperitoneal injection groups are 7971.935 ± 311.686 %ID min mL^{-1} (*i.v.*) and 1919.651 ± 132.7 %ID min mL^{-1} (*i.p.*), respectively (Table II, groups 1 and 2). These AUC data show that only approximately a quarter of the intraperitoneal administrated PE enters the blood circulation. Figure 2b shows that, happened as general, the intravenous administered PE accumulates into the liver and spleen rapidly due to the MPS. Meanwhile, the PE shows a blood clearance (Fig. 2a). The result in Fig. 2b presents a good agreement with the blood clearance in Fig. 2a. For the intraperitoneal administered PE, it preferentially remains in the injection site (Fig. 2b) and the fluorescence intensity experiences a slight decrease (Fig. 2b) which is consistent with the increase observed in Fig. 2a. For better analysis of tissue distribution of the intraperitoneal administered PE, we increased the intraperitoneal injection dose from 5 μmol phospholipid·kg^{-1} to 20 μmol phospholipid·kg^{-1}. Figure 2c shows that the intraperitoneal administered PE is gradually accumulated into lymph nodes, thymus, spleen, and liver. At 30 min post-injection, no fluorescent signal is detected for all of them. At 60 min post-injection, strong signals are detected in mesenteric lymph nodes, spleen, and liver. For the thymus, submaxillary lymph nodes, and popliteal lymph nodes which are

a

	PE-B	PE
Composition	MCT/E80/mPEG$_{2000}$-DSPE (75.31/17.62/7.07, *w/w*)	DiR/MCT/E80/mPEG$_{2000}$-DSPE (3.21/72.89/17.05/6.85, *w/w*)
Diameter (nm)	139.3 ± 3.7	147.3 ± 4.2
P.I.	0.1692 ± 0.023	0.1761 ± 0.008
Zeta potential (mV)	-29.82 ± 3.19	-26.17 ± 2.85

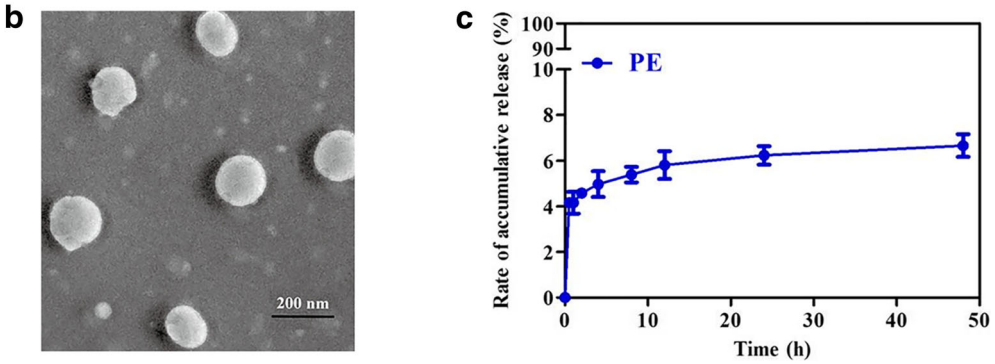

Fig. 1. The characteristics of the PE. **a** The composition, diameter and *zeta* potential of the PE-B and PE. The P.I. values of each group represent the particle size distribution. **b** The TEM image of the PE prepared at an accelerating voltage of 200 kV. Scale bar = 200 nm. **c** The drug release curve of the PE. Data is shown as means ± standard deviation

away from the peritoneal cavity, the signals are also detected, but the intensities are not strong. Up to 240 min, the signals of all groups are significantly increased especially the spleen and liver. Therefore, it can be verified that the PE can gain access to the whole lymphatic circulatory system and the lymphatic circulation eventually returns this lymph to the blood circulation. Upon reaching the blood circulation, PE appears to be treated in an identical fashion as intravenous administered PE and the blood circulating PE can also accumulate into the liver and spleen. Furthermore, using the Carestream Molecular Imaging Systems software, the ROI analysis of mean fluorescent intensity in the spleen and liver reveals that the spleen has much higher accumulation than the liver (mean intensity, 2078.251 ± 92.343, 1754.939 ± 114.714, $^{**}p = 0.032$).

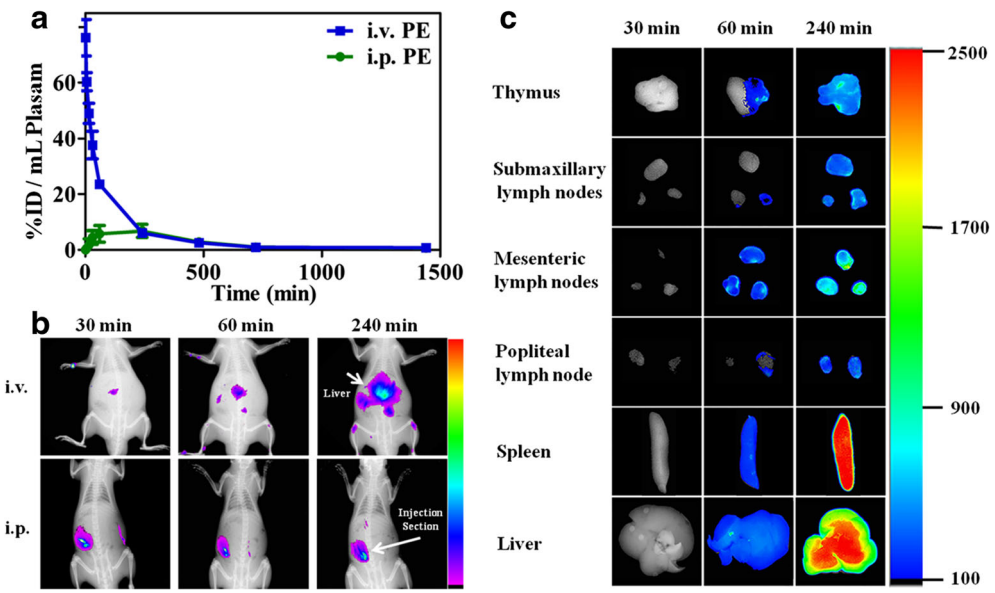

Fig. 2. The pharmacokinetics and tissue distribution of the PE administered by intravenous or intraperitoneal injection. **a** PE (5 μmol phospholipid·kg^{-1}) was administered to rats intravenously or intraperitoneally ($n = 6$). The plasma DiR concentration-time curves are shown as means ± standard deviation. **b** PE (5 μmol phospholipid·kg^{-1}) was administered intravenously or intraperitoneally to rats ($n = 6$). After the injection, the *in situ* tissue distribution was analyzed by *in vivo* fluorescent imaging method. **c** PE (20 μmol phospholipid·kg^{-1}) was administered intraperitoneally to rats ($n = 6$). After the injection, the *in vitro* tissue distribution was analyzed by *in vivo* fluorescent imaging method

The ABC Phenomenon of the Intravenous/Intraperitoneal Injected PEGylated Nanoemulsions

The intravenous injection method is widely used in the field of study the ABC phenomenon and only a few literatures using the subcutaneous injection method have been reported. In this study, we firstly used the intraperitoneal injection method to investigate the ABC phenomenon. The experimental protocol can be found in Table II and in the "MATERIALS AND METHODS" section. In brief, rats were treated with the PE-B at 0.5, 5, 50, or 100 μmol phospholipid·kg^{-1} using intravenous/intraperitoneal injection method. Seven days later, 5 μmol phospholipid·kg^{-1} PE was intravenously administered. As shown in Fig. 3, the ABC phenomenon can be induced with PE-B nanoemulsions by intravenous (Fig. 3a) and intraperitoneal (Fig. 3b) injections. Increasing the lipid concentration, the pharmacokinetic profiles of the second administration PE can be gently influenced (Fig. 3). The lipid dose of 5 μmol phospholipid·kg^{-1} induces the strongest ABC phenomenon ($AUC_{(0-\infty)}$, 847.192 ± 28.484 %ID min mL^{-1} for 0.5 μmol phospholipid·kg^{-1} (*i.v.*) and 752.998 ± 29.574 %ID min mL^{-1} for 5 μmol phospholipid·kg^{-1} (*i.v.*), $^{**}p = 0.028$; 1530.188 ± 73.831 %ID min mL^{-1} for 0.5 μmol phospholipid·kg^{-1} (*i.p.*) and 1163.238 ± 30.513 %ID min mL^{-1} for 5 μmol phospholipid·kg^{-1} (*i.p.*), $^{**}p = 0.015$). Compared with the intravenous injection, the intraperitoneal injection induces a slightly weaker extent of the ABC phenomenon (ABC index, 0.12 for 5 μmol phospholipid·kg^{-1} (*i.v.*) and 0.18 for 5 μmol phospholipid·kg^{-1} (*i.p.*)). The ABC indexes of each group are summarized in Table II.

The Effects of Intraperitoneal Pre-injection of Sterile Water

For further investigating the ABC phenomenon induced by intraperitoneal injected PE-B, intraperitoneal pre-injection of sterile water method was used. Detailed experimental schemes can be found in Table II and "MATERIALS AND METHODS" section. As shown in Fig. 4a and Table II, the data of the schemes *i.v.* PE and *i.p.* water–*i.v.* PE (groups 3 and 12 in Table II) shows that the pre-intraperitoneal administration sterile water cannot influence the pharmacokinetics of the intravenous injected PE ($AUC_{(0-\infty)}$, 7465.912 ± 312.166 %ID min mL^{-1}, 7601.000 ± 141.299 %ID min mL^{-1}, $p = 0.565$). Then, the result of the schemes *i.v.* PE-B–*i.v.* PE and *i.p.* water–*i.v.* PE-B–*i.v.* PE (groups 5 and 13 in the Table II) suggests that the pre-peritoneal administration sterile water cannot influence the ABC phenomenon induced by the intravenous injected PE-B ($AUC_{(0-\infty)}$, 752.998 ± 29.574 %ID min mL^{-1}, 782.294 ± 32.129 %ID min mL^{-1}, $p = 0.329$). However, for the schemes *i.p.* PE-B–*i.v.* PE and *i.p.* water–*i.p.* PE-B–*i.v.* PE (groups 9 and 14 in the Table II), we got significant different results that the pre-peritoneal administration sterile water can obviously inhibit the ABC phenomenon ($AUC_{(0-\infty)}$, 1163.238 ± 30.513 %ID min mL^{-1}, 3168.367 ± 79.186 %ID min mL^{-1}, $^{***}p = 0.0006$). Furthermore, the productions of anti-PEG IgM (group 1, group 2, and group 14 in Table II) were measured. The detailed experimental protocol can be found in the "Electronic Supplementary Information". As shown in Fig. 4b, the schemes *i.v.* PE, *i.p.* PE, and *i.p.* water–*i.p.* PE feature nearly same levels of anti-PEG IgM.

Peritoneal Fluid Smear

Cells smears are used to study the characteristic morphologies of the immune cells extracted from peritoneal lavage fluid under an optical microscope. The detailed experiment method is shown in the Electronic Supplementary Information. As described in many literatures, different immune cells display various morphologies under microscope (35,36): lymphocytes have a large nucleus occupying most of the cytoplasm; monocytes feature typical bean-shaped nucleus; neutrophils show a distinctive multilobed nucleus; tissue eosinophils have bright purple-red particles on the surface and mast cells possess large amounts of dark blue particles on their surface. Thusly, as shown in Fig. 5, the total immune cells count significantly increase after the pre-intraperitoneal administered of sterile water, and the mast cells disappear.

Table II. The Injection Protocols and the Pharmacokinetics of the PE

Group	Pretreatment	First dose	Test dose (5 μmol phospholipid·kg^{-1})	The pharmacokinetics of PE		
				$AUC_{(0-\infty)}$ (%ID min mL^{-1})	C_{max} (%ID mL^{-1})	ABC index
1	–	–	PE (*i.p.*)	1919.651 ± 132.737	6.798 ± 1.172	–
2	–	–	PE (*i.v.*)	7971.935 ± 311.686	85.007 ± 3.592	–
3	–	5%Glu	PE (*i.v.*)	7465.912 ± 312.166	79.564 ± 2.965	–
4	–	PE-B (0.5 μmol phospholipid·kg^{-1}, *i.v.*)	PE (*i.v.*)	847.192 ± 28.484	37.228 ± 1.924	0.13
5	–	PE-B (5 μmol phospholipid·kg^{-1}, *i.v.*)	PE (*i.v.*)	752.998 ± 29.574	19.764 ± 1.289	0.12
6	–	PE-B (50 μmol phospholipid·kg^{-1}, *i.v.*)	PE (*i.v.*)	276.208 ± 64.369	40.216 ± 2.507	0.20
7	–	PE-B (100 μmol phospholipid·kg^{-1}, *i.v.*)	PE (*i.v.*)	1896.347 ± 88.770	53.803 ± 3.602	0.29
8	–	PE-B (0.5 μmol phospholipid·kg^{-1}, *i.p.*)	PE (*i.v.*)	1530.188 ± 73.831	31.888 ± 4.225	0.24
9	–	PE-B (5 μmol phospholipid·kg^{-1}, *i.p.*)	PE (*i.v.*)	1163.238 ± 30.513	33.554 ± 5.950	0.18
10	–	PE-B (50 μmol phospholipid·kg^{-1}, *i.p.*)	PE (*i.v.*)	1669.306 ± 75.773	49.203 ± 4.257	0.26
11	–	PE-B (100 μmol phospholipid·kg^{-1}, *i.p.*)	PE (*i.v.*)	2366.885 ± 113.768	65.362 ± 3.079	0.37
12	Water (*i.p.*)	5%Glu	PE (*i.v.*)	7601.000 ± 141.299	93.057 ± 7.989	–
13	Water (*i.p.*)	PE-B (5 μmol phospholipid·kg^{-1}, *i.v.*)	PE (*i.v.*)	782.294 ± 32.129	23.532 ± 4.257	0.10
14	Water (*i.p.*)	PE-B (5 μmol phospholipid·kg^{-1}, *i.p.*)	PE (*i.v.*)	3168.367 ± 79.186	64.148 ± 5.293	0.42

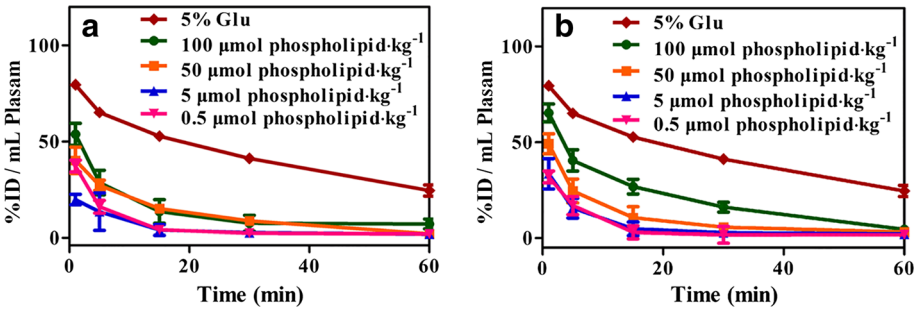

Fig. 3. The ABC phenomenon induced by intravenous/intraperitoneal administrated the PE. The PE-B in different lipid concentrations (0.5, 5, 50, and 100 μmol phospholipid·kg^{-1}) was injected **a** intravenously or **b** intraperitoneally to rats ($n = 6$). Seven days later, the PE (5 μmol phospholipid·kg^{-1}) was administered similarly. After the injection, the plasma pharmacokinetic profile of the second injection of the PE was studied. All data is shown as the means ± standard deviation

DISCUSSION

Pharmacokinetics of the Intravenous/Intraperitoneal Injected PE

As shown in Fig. 2a, the pharmacokinetics curve of the intraperitoneal administered PE features a gentle absorption peak (at 4 h, C_{max} 6.798 ± 1.172 %ID mL^{-1}) which implies that the PE is not easy to enter into the blood circulation from peritoneal cavity. As reported, the width of gap junctions in normal endothelia is typically smaller than 6 nm (37) and thusly the intraperitoneal administered PE (~ 140 nm) cannot enter into the blood circulation through the portal or the systemic circulation directly. Another possible way to enter into the blood is through the lymphatic circulatory system. Figure 2c shows that at 60 min after the intraperitoneal administration, the florescence intensity of draining mesenteric lymph node is strong while thymus and other lymph nodes (submaxillary lymph nodes and popliteal lymph nodes) present low intensities. Up to 240 min, all of their florescence intensities are significantly increased. Therefore, it can be deduced that the intraperitoneal administered PE gain access to the lymphatic circulatory and thus increase the florescence intensity in immune organs and lymph nodes. Subsequently, the PE will flow into the blood circulatory. The process is that the intraperitoneal administered PE can be accumulated by the draining mesenteric lymph nodes to form the lymph. The lymph then flows to the other nearest lymph nodes (popliteal or submaxillary lymph nodes) by lymphatics. The lymphatic circulation eventually transports this lymph to blood, chiefly *via* the thoracic duct. Then, the PE will gradually accumulate into the liver and spleen after them entering the blood circulation.

Unlike the blood which is driven by a dedicated pump, the lymph flows comparatively sluggish by the continual movements of one part of the body with respect to another and eventually *via* one-way valves enters the blood circulation (38). Based on this common property of lymphatic circulation, we can speculate that the spleen and liver should not have high accumulations. However, the ROI analysis of the mean fluorescent intensity reveals that the accumulations in both of the spleen and of the liver are very high at 60 min post-injection. Therefore, other special pathways should exist to transport the PE from abdominal cavity to the liver and spleen. Some literatures state that fully mature macrophages in peritoneal cavity rapidly make inroads into injured liver by non-vascular route recruitment across the mesothelium mature peritoneal cavity (39). Hence, it is conceived that a direct route exists for the mature peritoneal cavity macrophages taking up the intraperitoneal injected PEGylated nanoemulsions and then transport it into the liver and spleen rapidly at 60 min. In addition, due to the spleen is a huge

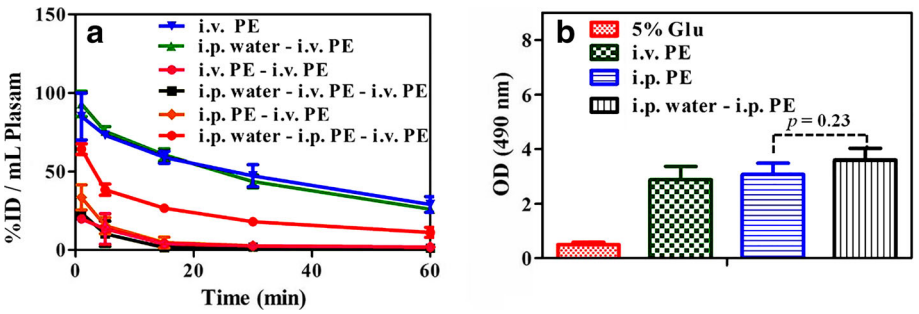

Fig. 4. The influence of pre-intraperitoneal injection of sterile water on the ABC phenomenon and the secretion of anti-PEG IgM. The 54 mL kg^{-1} sterile water was intraperitoneally administered to rats ($n = 6$). Two days later, the 5 μmol phospholipid·kg^{-1} PE-B was intravenously/intraperitoneally administered to rats depending on assigned group ($n = 6$). Seven days later, **a** the PE (5 μmol phospholipid·kg^{-1}) was intravenously administered again and the plasma pharmacokinetic profile of the second injection of the PE was studied or **b** the blood was collected to analyze the secretion of anti-PEG IgM. All data is shown as the means ± standard deviation

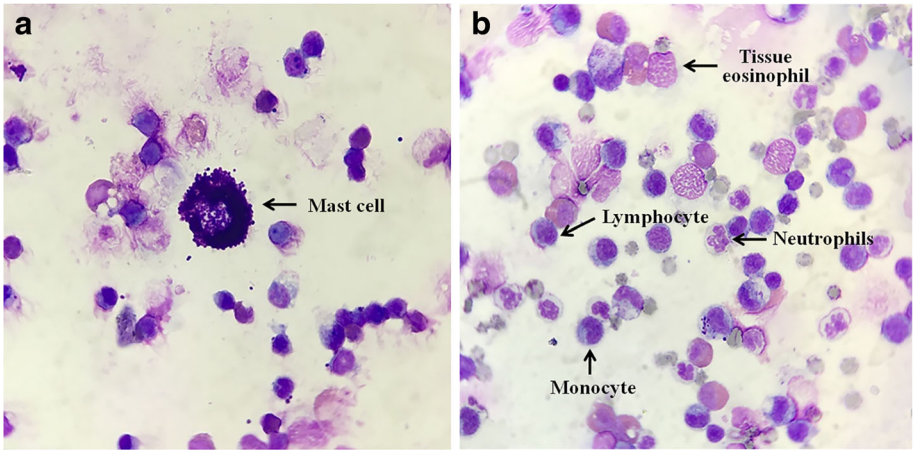

Fig. 5. Sterile water (54 mL kg^{-1}) was intraperitoneally administered to rats ($n = 3$). A control group was pre-intraperitoneally injected with the same amount of 5% Glu. Two days later, rats were anesthetized and intraperitoneally injected with PBS (40 mL kg^{-1}). The immune cells from peritoneal lavage fluid were observed under a microscope using ×10 eyepiece and ×100 oil immersion objectives. **a** A normal peritoneal lavage fluid smear. The immune cells with dark blue particles are the mast cells. **b** A smear from a peritoneal lavage collected from a rat that underwent sterile water pretreatment

immune organ on the lymph circulation, the spleen presents significant higher accumulation than the liver at 240 min post-injection (**$p = 0.032$).

The ABC Phenomenon of the Intravenous/Intraperitoneal Injected PE

Compared with the intravenous injection method, the intraperitoneal injection method has some unique advantages. First of all, the pharmacokinetic advantage of the intraperitoneal chemotherapeutics has a significant higher concentration in the abdominal cavity (40,41). The second has feature of laparoscopic hyperthermic intraperitoneal chemotherapy as an important option in the field of management digestive tract or uterus cancers with peritoneal carcinomatosis (42,43). Furthermore, intraperitoneal immunotherapy also can be used in patients with peritoneal metastases as an innovative and promising method (44,45). In addition, intraperitoneal injection method is always used to investigate the immune system (46). However, no reports pay attention to the ABC phenomenon induced by intraperitoneal administrated nanoparticles.

In this study, we firstly propose that the intraperitoneal administration method can also induce the ABC phenomenon. The pharmacokinetic profiles of the second intravenously injected PE are influenced by lipid concentration (Fig. 3). For both of intravenous and intraperitoneal injection methods, the strongest ABC phenomenon is induced at the dose of 5 μmol phospholipid·kg^{-1}. In addition, Ishida et al. demonstrated that intravenous injection of 0.001 μmol phospholipid·kg^{-1} PEGylated liposomes can induce the strongest extent of the ABC phenomenon (25). Hence, it is suggested that for the PEGylated nanoemulsions and the PEGylated liposomes, the most appropriate stimulus to the ABC phenomenon comes from different lipid injection doses. In addition, for the PEGylated nanoemulsions, PEGylated solid lipid nanoparticles (23), and the conventional liposomes (7,25), 5 μmol phospholipid·kg^{-1} is their most appropriate stimulation dose to induce the strongest extend of the ABC phenomenon.

The ABC index values of the intraperitoneal/intravenous injection group are 0.18 and 0.12 respectively. Our previous studies have revealed that the ABC phenomenon can be induced by subcutaneous administration of the PEGylated nanoparticles. The ABC phenomenon induced by the foot injection is stronger than that by the nape administration. The ABC index values of the foot/nape injection group are 0.24 and 0.60 respectively. Thus, it can be extrapolated that different injection methods give rise to different extents of the ABC phenomenon. The PEGylated nanocarriers injected by intravenous, intraperitoneal, and subcutaneous methods will encounter different kinds of cells or tissues and enter the blood circulation by different manners. Hence, all the cells, organs, and the blood/lymph circulation in the body they encountered after the injection have potential to influence the ABC phenomenon.

The Effects of the Intraperitoneal Pre-injection of Sterile Water

Through a series of experiments, we find that the ABC phenomenon is significantly inhibited by pre-peritoneal administration of sterile water, as shown in Fig. 4a. Ishida et al. suggested a convincing mechanism that the amount of anti-PEG IgM has a positive relationship with the magnitude of the ABC phenomenon (17). Specifically, anti-PEG IgM is secreted by splenic B cells in response to the first injected PEGylated nanocarriers; when the animal receives the second administrated PEGylated nanocarriers, the anti-PEG IgM can quickly recognized the re-injected nanocarriers and thus causes the rapid clearance of the second dose from the blood circulation (16). Because of the importance of anti-PEG IgM on the induction of the ABC phenomenon, it is necessary to measure the secretion of the anti-PEG IgM. Figure 4b describes the anti-PEG IgM before and after the pre-peritoneal administration of sterile water. Obviously, pre-peritoneal administration of sterile water does not decrease

the anti-PEG IgM secretion. This result is unexpected because attenuate ABC phenomenon should be in corresponding to low production of anti-PEG IgM. Mathias Heikenwalder et al. reported (47) that rats were repeated intraperitoneal treated with cytidyl guanosyl-containing oligodeoxynucleotides (CpG-ODN) for 2–20 days and immunosuppression occurred in rats along with the spleen, mesenteric lymph nodes, and inguinal lymph nodes significantly hyperplastic. However, serum IgM antibody titers cannot be influenced by repeated intraperitoneal treated with CpG-ODN. Hence, for our work, the fact that the anti-PEG IgM secretion cannot be affected by pre-peritoneal administration of sterile water is a reasonable result.

In order to further study the reason why the ABC phenomenon can be significantly inhibited by the pre-peritoneal injection of sterile water, while the anti-PEG IgM secretes at the same level, the immune cells in the peritoneal cavity were investigated by peritoneal fluid smear method. As shown in Fig. 5, although the amount of the immune cells increases significantly, mast cells in the peritoneal cavity disappear. The mast cells in the serosal cavity support underlying thymus-independent type (TI) immunity (48) and PEGylated nanoparticles as a TI-2 antigen might be recognized by splenic B cells (17). Hence, the mast cells have potential to influence the ABC phenomenon.

As reported, mast cells can release histamines and different kinds of cytokine mediators (49). In this work, the mast cells are physical destroyed by peritoneal administration of sterile water and, as a result, subsequently release their cell contents including cytokine mediators into the peritoneal cavity. Different cytokine mediators behave different functions. Some cytokine mediators can recruit other immune cells into specific region (50). This is the reason why we can observe significant increase in amount of the immune cells, while mast cells disappear (Fig. 5). Some other cytokine mediators can induce immunosuppression (51) which decrease the interaction of the PE-B with immune cells such as dendritic cells, then decrease the transportation of the PE-B to lymph nodes, and finally inhibit the ABC phenomenon. Hence, we suggest that the disappearance of mast cells is probably responsible for the attenuated ABC phenomenon.

CONCLUSION

In summary, our results firstly reveal that the ABC phenomenon can be induced by intraperitoneal administered PEGylated nanoemulsions. The tissue distributions (*in vivo* or *in vitro*) of the first injected PE by intraperitoneal injection suggest that the PE gains access to the whole lymphatic circulatory system. Interestingly, the ABC phenomenon induced by intraperitoneal injected PE-B can be significantly inhibited by intraperitoneal pre-injection of distilled water. For further understanding this issue, the characteristic morphologies of immune cells were studied. We suggest that the rapid depletion of mast cells in peritoneal cavity should be responsible for the decrease of the ABC phenomenon.

FUNDING INFORMATION

This research was aided financially by the National Natural Science Foundation of China (Grant Nos. 81072602, 81373334).

REFERENCES

1. Soppimath KS, Aminabhavi TM, Kulkarni AR, Rudzinski WE. Biodegradable polymeric nanoparticles as drug delivery devices. J Control Release. 2001;70(1–2):1–20.
2. Singh R, Lillard JW Jr. Nanoparticle-based targeted drug delivery. Exp Mol Pathol. 2009;86(3):215–23.
3. Mainardes RM, Silva LP. Drug delivery systems: past, present, and future. Curr Drug Targets. 2004;5(5):449–55.
4. Bunker A, Magarkar A, Viitala T. Rational design of liposomal drug delivery systems, a review: combined experimental and computational studies of lipid membranes, liposomes and their PEGylation. Biochim Biophys Acta. 2016;1858(10):2334–52.
5. Jokerst JV, Lobovkina T, Zare RN, Gambhir SS. Nanoparticle PEGylation for imaging and therapy. Nanomedicine. 2011;6(4):715–28.
6. Dams ET, Laverman P, Oyen WJ, Storm G, Scherphof GL, van der Meer JW, et al. Accelerated blood clearance and altered biodistribution of repeated injections of sterically stabilized liposomes. J Pharmacol Exp Ther. 2000;292(3):1071–9.
7. Laverman P, Carstens MG, Boerman OC, Dams ETM, Oyen WJ, van Rooijen N, et al. Factors affecting the accelerated blood clearance of polyethylene glycol-liposomes upon repeated injection. J Pharmacol Exp Ther. 2001;298(2):607–12.
8. Ishida T, Maeda R, Ichihara M, Mukai Y, Motoki Y, Manabe Y, et al. The accelerated clearance on repeated injection of pegylated liposomes in rats: laboratory and histopathological study. Cell Mol Biol Lett. 2002;7(2):286.
9. Lila ASA, Kiwada H, Ishida T. The accelerated blood clearance (ABC) phenomenon: clinical challenge and approaches to manage. J Control Release. 2013;172(1):38–47.
10. Im H-J, England CG, Feng L, Graves SA, Hernandez R, Nickles RJ, et al. Accelerated blood clearance phenomenon reduces the passive targeting of PEGylated nanoparticles in peripheral arterial disease. ACS Appl Mater Interfaces. 2016;8(28):17955–63.
11. Ishihara T, Takeda M, Sakamoto H, Kimoto A, Kobayashi C, Takasaki N, et al. Accelerated blood clearance phenomenon upon repeated injection of PEG-modified PLA-nanoparticles. Pharm Res. 2009;26(10):2270–9.
12. Zhao Y, Wang L, Yan M, Ma Y, Zang G, She Z, et al. Repeated injection of PEGylated solid lipid nanoparticles induces accelerated blood clearance in mice and beagles. Int J Nanomedicine. 2012;7:2891.
13. Koide H, Asai T, Hatanaka K, Urakami T, Ishii T, Kenjo E, et al. Particle size-dependent triggering of accelerated blood clearance phenomenon. Int J Pharm. 2008;362(1–2):197–200.
14. Shiraishi K, Yokoyama M. Polymeric micelles possessing polyethyleneglycol as outer shell and their unique behaviors in accelerated blood clearance phenomenon. Biol Pharm Bull. 2013;36(6):878–82.
15. Środa K, Rydlewski J, Langner M, Kozubek A, Grzybek M, Sikorski AF. Repeated injections of PEG-PE liposomes generate anti-PEG antibodies. Cell Mol Biol Lett. 2005;10:37–47.
16. Ishida T, Ichihara M, Wang X, Kiwada H. Spleen plays an important role in the induction of accelerated blood clearance of PEGylated liposomes. J Control Release. 2006;115(3):243–50.
17. Ishida T, Ichihara M, Wang X, Yamamoto K, Kimura J, Majima E, et al. Injection of PEGylated liposomes in rats elicits PEG-specific IgM, which is responsible for rapid elimination of a second dose of PEGylated liposomes. J Control Release. 2006;112(1):15–25.
18. Shimizu T, Ishida T, Kiwada H. Transport of PEGylated liposomes from the splenic marginal zone to the follicle in the induction phase of the accelerated blood clearance phenomenon. Immunobiology. 2013;218(5):725–32.
19. Ishida T, Wang X, Shimizu T, Nawata K, Kiwada H. PEGylated liposomes elicit an anti-PEG IgM response in a T cell-independent manner. J Control Release. 2007;122(3):349–55.
20. Ishida T, Kashima S, Kiwada H. The contribution of phagocytic activity of liver macrophages to the accelerated blood clearance (ABC) phenomenon of PEGylated liposomes in rats. J Control Release. 2008;126(2):162–5.

21. Shimizu T, Mima Y, Hashimoto Y, Ukawa M, Ando H, Kiwada H, et al. Anti-PEG IgM and complement system are required for the association of second doses of PEGylated liposomes with splenic marginal zone B cells. Immunobiology. 2015;220(10):1151–60.
22. Wang L, Su Y, Wang X, Liang K, Liu M, Tang W, et al. Effects of complement inhibition on the ABC phenomenon in rats. Asia J Pharmaceut Sci. 2017;12(3):250–8.
23. Zhao Y, Wang C, Wang L, Yang Q, Tang W, She Z, et al. A frustrating problem: accelerated blood clearance of PEGylated solid lipid nanoparticles following subcutaneous injection in rats. Eur J Pharm Biopharm. 2012;81(3):506–13.
24. Ishida T, Ichikawa T, Ichihara M, Sadzuka Y, Kiwada H. Effect of the physicochemical properties of initially injected liposomes on the clearance of subsequently injected PEGylated liposomes in mice. J Control Release. 2004;95(3):403–12.
25. Ishida T, Harada M, Wang XY, Ichihara M, Irimura K, Kiwada H. Accelerated blood clearance of PEGylated liposomes following preceding liposome injection: effects of lipid dose and PEG surface-density and chain length of the first-dose liposomes. J Control Release. 2005;105(3):305–17.
26. Peng K-W, TenEyck CJ, Galanis E, Kalli KR, Hartmann LC, Russell SJ. Intraperitoneal therapy of ovarian cancer using an engineered measles virus. Cancer Res. 2002;62(16):4656–62.
27. Di Giorgio A, Naticchioni E, Biacchi D, Sibio S, Accarpio F, Rocco M, et al. Cytoreductive surgery (peritonectomy procedures) combined with hyperthermic intraperitoneal chemotherapy (HIPEC) in the treatment of diffuse peritoneal carcinomatosis from ovarian cancer. Cancer. 2008;113(2):315–25.
28. Gill RS, Al-Adra DP, Nagendran J, Campbell S, Shi X, Haase E, et al. Treatment of gastric cancer with peritoneal carcinomatosis by cytoreductive surgery and HIPEC: a systematic review of survival, mortality, and morbidity. J Surg Oncol. 2011;104(6):692–8.
29. Williamson SK, Johnson GA, Maulhardt HA, Moore KM, McMeekin D, Schulz TK, et al. A phase I study of intraperitoneal nanoparticulate paclitaxel (Nanotax®) in patients with peritoneal malignancies. Cancer Chemother Pharmacol. 2015;75(5):1075–87.
30. Moreno-Aspitia A, Perez EA. Nanoparticle albumin-bound paclitaxel (ABI-007): a newer taxane alternative in breast cancer. Future Oncol. 2005;1(6):755–62.
31. Lu Z, Tsai M, Lu D, Wang J, Wientjes MG, JL-S A. Tumor-penetrating microparticles for intraperitoneal therapy of ovarian cancer. J Pharmacol Exp Ther. 2008;327(3):673–82.
32. Xu S, Fan H, Yin L, Zhang J, Dong A, Deng L, et al. Thermosensitive hydrogel system assembled by PTX-loaded copolymer nanoparticles for sustained intraperitoneal chemotherapy of peritoneal carcinomatosis. Eur J Pharm Biopharm. 2016;104:251–9.
33. Allen TM, Cullis PR. Liposomal drug delivery systems: from concept to clinical applications. Adv Drug Deliv Rev. 2013;65(1):36–48.
34. Liang K, Wang L, Su Y, Liu M, Feng R, Song Y, et al. Comparison among different "revealers" in the study of accelerated blood clearance phenomenon. Eur J Pharm Sci. 2018;114:210–6.
35. Yen-Rei AY, O'Koren EG, Hotten DF, Kan MJ, Kopin D, Nelson ER, et al. A protocol for the comprehensive flow cytometric analysis of immune cells in normal and inflamed murine non-lymphoid tissues. PLoS One. 2016; https://doi.org/10.1371/journal.pone.0150606.
36. Horny H-P, Sotlar K, Valent P. Mastocytosis: immunophenotypical features of the transformed mast cells are unique among hematopoietic cells. Immunol Allergy Clin North Am. 2014;34(2):315–21.
37. Drummond DC, Meyer O, Hong K, Kirpotin DB, Papahadjopoulos D. Optimizing liposomes for delivery of chemotherapeutic agents to solid tumors. Pharmacol Rev. 1999;51(4):691–744.
38. Dobrovolskaia MA, McNeil SE. Handbook of immunological properties of engineered nanomaterials. 3rd ed. World Scientific: CRC Press; 2013.
39. Wang J, Kubes P. A reservoir of mature cavity macrophages that can rapidly invade visceral organs to affect tissue repair. Cell. 2016;165(3):668–78.
40. Tewari D, Java JJ, Salani R, Armstrong DK, Markman M, Herzog T, et al. Long-term survival advantage and prognostic factors associated with intraperitoneal chemotherapy treatment in advanced ovarian cancer: a gynecologic oncology group study. J Clin Oncol. 2015;33(13):1460–6.
41. Sadeghi B, Arvieux C, Glehen O, Beaujard AC, Rivoire M, Baulieux J, et al. Peritoneal carcinomatosis from non-gynecologic malignancies. Cancer. 2000;88(2):358–63.
42. Yonemura Y, Ishibashi H, Hirano M, Mizumoto A, Takeshita K, Noguchi K, et al. Effects of neoadjuvant laparoscopic hyperthermic intraperitoneal chemotherapy and neoadjuvant intraperitoneal/systemic chemotherapy on peritoneal metastases from gastric cancer. Ann Surg Oncol. 2017;24(2):478–85.
43. Gesson-Paute A, Ferron G, Thomas F, de Lara EC, Chatelut E, Querleu D. Pharmacokinetics of oxaliplatin during open versus laparoscopically assisted heated intraoperative intraperitoneal chemotherapy (HIPEC): an experimental study. Ann Surg Oncol. 2008;15(1):339–44.
44. Goéré D, Gras-Chaput N, Aupérin A, Flament C, Mariette C, Glehen O, et al. Treatment of gastric peritoneal carcinomatosis by combining complete surgical resection of lesions and intraperitoneal immunotherapy using catumaxomab. BMC Cancer. 2014;14(1):148–55.
45. Deraco M, Rossi CR, Pennacchioli E, Guadagni S, Somers DC, Santoro N, et al. Cytoreductive surgery followed by intraperitoneal hyperthermic perfusion in the treatment of recurrent epithelial ovarian cancer: a phase II clinical study. Tumori. 2001;87(3):120–6.
46. Beutler B, Milsark I, Cerami A. Passive immunization against cachectin/tumor necrosis factor protects mice from lethal effect of endotoxin. Science. 1985;229(4716):869–71.
47. Heikenwalder M, Polymenidou M, Junt T, Sigurdson C, Wagner H, Akira S, et al. Lymphoid follicle destruction and immunosuppression after repeated CpG oligodeoxynucleotide administration. Nat Med. 2004;10(2):187–92.
48. MacQueen G, Marshall J, Perdue M, Siegel S, Bienenstock J. Pavlovian conditioning of rat mucosal mast cells to secrete rat mast cell protease II. Science. 1989;243(4887):83–5.
49. Galli SJ, Nakae S, Tsai M. Mast cells in the development of adaptive immune responses. Nat Immunol. 2005;6(2):135–42.
50. Jatana S, Palmer BC, Phelan SJ, DeLouise LA. Immunomodulatory effects of nanoparticles on skin allergy. Sci Rep. 2017;7(1):3979–89.
51. Galli SJ, Grimbaldeston M, Tsai M. Immunomodulatory mast cells: negative, as well as positive, regulators of immunity. Nat Rev Immunol. 2008;8(6):478–86.